Bioderived Rotaxanes via Dynamic Covalent Boron Chemistry

Jingjing Yu[1], Marius Gaedke[1], Satyajit Das[1], Daniel L. Stares[2], Christoph A. Schalley[2], Fredrik Schaufelberger[1]*

[1] KTH Royal Institute of Technology, Department of Chemistry, Teknikringen 30, 10044 Stockholm, Sweden

[2] Institut für Chemie und Biochemie, Freie Universität Berlin, Arnimallee 20, 14195 Berlin, Germany.

Keywords: Mechanical bonds, rotaxanes, dynamic covalent chemistry, boronic acids, self-assembly.

ABSTRACT

We report on the use of vicinal diols as a template for synthesis of mechanically interlocked molecules. Vicinal diols are prevalent in bio(macro)molecules such as carbohydrates, RNA as well as polyhydroxylated natural products, and a range of methods exists for recognition and selective binding to these motifs. Here we use dynamic covalent boron chemistry to reversibly attach a V-shaped boronic acid pincer ligand with two alkene-appended arms to a linear diol-containing thread. Following condensation of the pincer ligand with the thread, ring-closing metathesis establishes a quasi[1]rotaxane architecture along with a non-entangled isomer in a 1:2 ratio. Advanced NMR spectroscopy and mass spectrometry unambiguously assigned the isomers and revealed that the quasi[1]rotaxane was in equilibrium with its hydrolyzed free [2]rotaxane form. The boron handle could also be selectively oxidized to kinetically trap the rotaxane in place. This study demonstrates that prevalent biomolecular motifs can be used as templates for establishing mechanical bonds, meaning it might be possible to interlock unmodified native biomolecules and biopolymers for future biomedical applications.

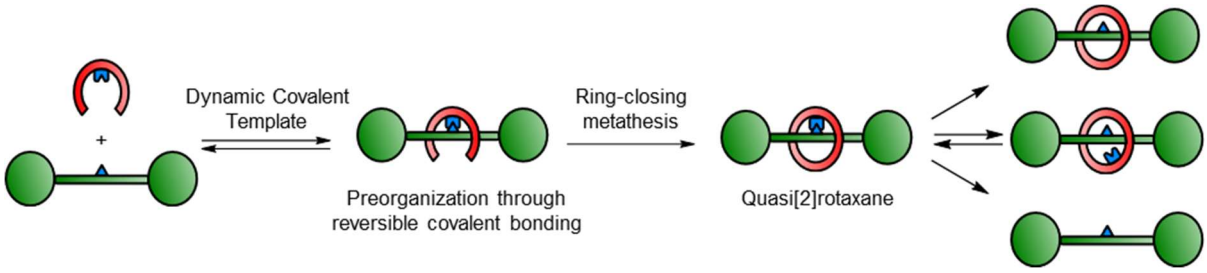

INTRODUCTION

Mechanically interlocked molecules (MIMs) such as rotaxanes, catenanes and molecular knots have long been considered challenging synthetic targets, but recent synthetic advances are now allowing their properties to be explored in greater detail and their applications to be probed more systematically.[1] One area that remains underdeveloped is the use of MIMs for biological applications.[2] MIMs are attractive functional units for chemical biology due to their dynamic nature and stimuli-responsiveness, in addition to how they sterically protect delicate functional groups against degradation. However, the community has only begun to scratch the surface of this rich and interesting field.[2a] From the sparse examples so far, MIMs have been used for small-molecule drug delivery[3], to protect sensitive imaging agents from degradation[4], for mechanical silencing of DNA duplex formation[5], to aid substrate passage through cell membranes[6], and for biosensing[7].

There are nevertheless significant barriers to applying MIMs in biological contexts, with the most substantial being the synthetic difficulty of making biocompatible (and water-soluble) molecules. Most synthetic routes towards MIMs rely on non-covalent interactions to pre-organize the individual

component before establishing the mechanical bond.[1a] However, this introduces extraneous functional groups (ligands for metals, H-bonds etc.) which are non-biogenic and cause problems in biological applications. A better approach would be to construct MIMs from biogenic building blocks, as such supramolecular assemblies would likely have higher biocompatibility.[8] Unfortunately, accessing molecules such as rotaxanes using biomolecules as templates is extremely difficult, as the biological environment disrupts most pre-organizing interactions and renders template effects weaker and less directional.

We hypothesized that covalent rather than non-covalent templates would be favorable for constructing MIMs with biologically relevant templates.[9] The robustness and directionality of covalent templates are higher than with non-covalent interactions, meaning mechanical bonds can be formed under more challenging conditions.[10] The use of covalent bonds to preorganize different molecular components before interlocking was established as far back as the 1960s[11] but most such strategies suffer limitations such as harsh cleavage conditions and complicated synthesis[9]. Here we report a straightforward approach to make [2]rotaxanes from bioderived building blocks via covalent templates (Scheme 1). Key to this method is the use of dynamic covalent chemistry to pre-organize a bioderived thread and a V-shaped pincer receptor into a conformation that delivers a rotaxane upon ring closure and cleavage of the dynamic covalent linkage.[12] Dynamic covalent bonds have "Goldilocks character" that make them uniquely suited as covalent templates, with the bonds being robust enough for efficient covalent template synthesis (under one set of conditions) but labile enough to later liberate the free MIM (under another set of conditions).[13]

Boronic esters are classic examples of dynamic covalent bonds and form by exchange between vicinal diols and boronic acids.[14] Reversible boronic acid complexation has been extensively used for biosensing[15], catalysis[16], self-healing materials[17] and to solubilize polysaccharides[18]. There is also ample precedence for the use of boron self-assembly to preorganize components towards macrocyclization[19], though dynamic boron chemistry has not seen much use for MIM synthesis[20]. Polyhydroxylated scaffolds and vicinal diols are furthermore ubiquitous in nature (RNA, carbohydrates, natural products etc.) and would hence provide versatile, naturally occurring templates for biocompatible rotaxanes.

This study establishes proof-of-concept for using dynamic boron chemistry and vicinal diol templates for [2]rotaxane synthesis. Our receptor uses a dynamic boron handle to reversibly bind to the hydroxyl groups, whilst apolar protruding side chains preorganize the receptor into a "clasp-type" conformation that encapsulates the top/bottom of the thread. This design causes clipping of the receptor onto the thread, and the dynamic covalent bond can then be readily broken or derivatized to free the quasi[1]rotaxane species and create true [2]rotaxanes.

RESULTS AND DISCUSSION

The V-shaped pincer ligand **1** bears a boronic acid moiety at its cleft and was synthesized in six steps as outlined in the Supporting information (Section S3). The ligand side chains were designed to feature benzyl-groups for increased dispersion interactions with the hydrophobic parts of the thread, to facilitate enclosure around rather than outside of the thread (*vide infra*).[21] As thread, we synthesized model compound **2** in five steps starting from the natural product tartaric acid. To ensure a stable thread architecture and facilitate synthesis, we used amide bonds to connect the tartrate unit to the stoppers. The pincer ligand **1** and thread **2** were mixed in anhydrous toluene, leading to spontaneous self-assembly of the dynamic boronic ester species **3** in 67-89% conversion, as determined by ^{1}H-NMR analysis (Figure 1, Table S1).[22] Pronounced ^{1}H-NMR spectral shifts for key resonances indicated successful complexation. For example, proton t_{10} shifts strongly downfield ($\Delta\delta$ = 0.7 ppm), while t_6 shifts upfield ($\Delta\delta$ = 0.2 ppm), indicating boronic ester formation and the arms of the pincer shielding the thread via the desired clasp-type conformation. Protons r_1, r_2, r_4 and r_5 on the pincer also shifts noticeably, again indicating a more rigidified environment along with boronic ester formation. Aside from an upfield shift of 0.4 ppm, proton r_3 also changes splitting pattern from singlet to a doublet of doublets, due to the diasterotopic protons now residing in a conformationally restricted chiral environment imposed by the tartrate chiral centers. ^{11}B-NMR spectroscopy gave a shift of 28.9 ppm for **3**, which supports assignment of the boron moiety as a trigonal boronic ester (Spectrum S26).[23] Reversibility of the linkage was confirmed by hydrolysing the complex back to **1** and **2** in water-saturated $CDCl_3$ (Figure S1-S2).

Scheme 1. Synthesis of a [2]rotaxane through a diol template.

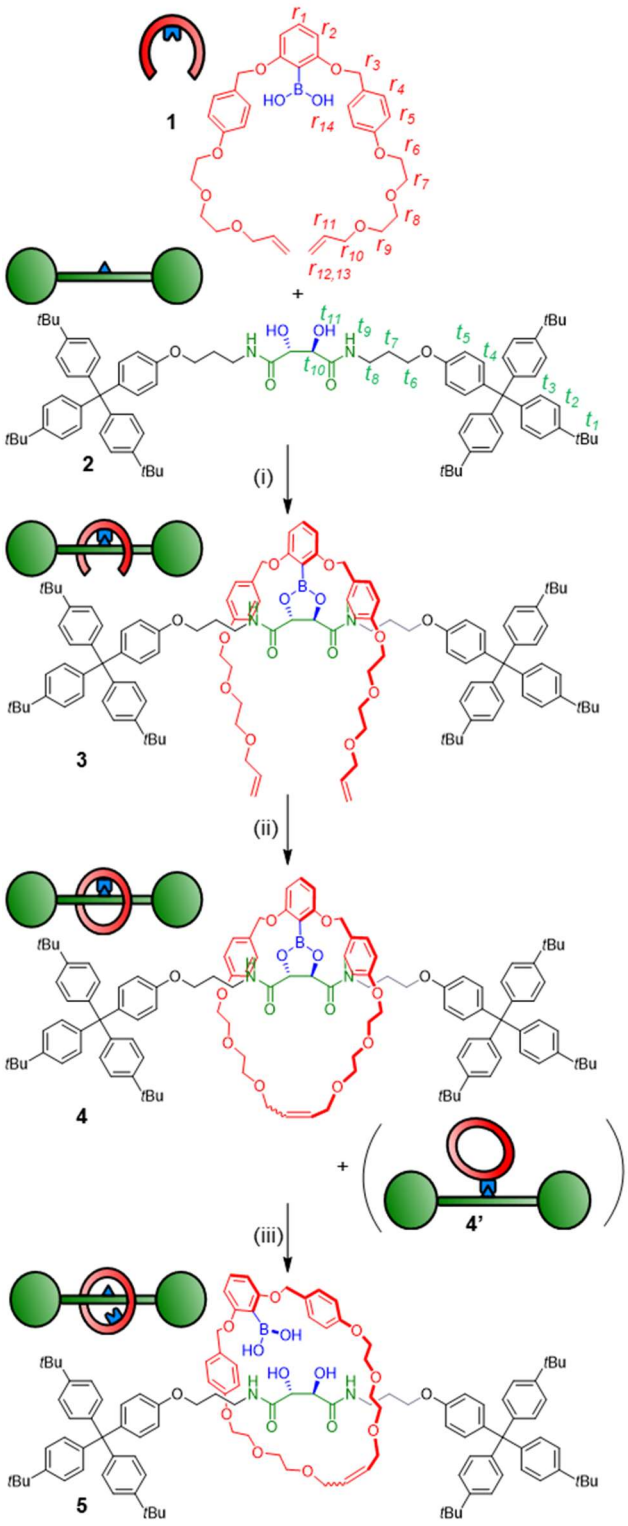

[a]Reagents and conditions: (i) **1** (1 equiv.), **2** (1 equiv.), toluene, RT, 24 h; (ii) Hoveyda-Grubbs 2nd generation catalyst, CH_2Cl_2, RT, 24 h (16% yield over two steps); (iii) H_2O, $CDCl_3$, RT, 7 d (equilibrium yield 70%).

The covalently linked clasp-type receptor **3** is preorganized for rotaxane formation via ring-closing metathesis (RCM).[24] While there is flexibility in the structure, that freedom of movement was deemed necessary for the arms to meet during ring closure as part of the RCM catalytic cycle (where an organometallic Ru complex is covalently attached to one chain terminus). [25] Indeed, treatment of complex **3** with Grubbs-Hoveyda 2nd generation catalyst in CH_2Cl_2 led to efficient ring closure, as

evidenced by ^{1}H-NMR spectra of the crude mixture (Figure S3). The majority of the crude reaction appeared to be composed of two ring-closed species in 2:1 ratio (the remainder being unidentified oligo- and polymeric species). Analysis using electrospray ionization high resolution mass spectrometry (ESI-HRMS) indicated both species had the same molecular mass (observed mass *m/z* 1817.0221 for $[C_{116}H_{139}N_2O_{14}+Na]^+$, calculated m/z 1817.0253) as the desired quasi[1]rotaxane product **4**. This led us to believe that the two compounds were structural isomers **4** and **4'** (Scheme 1), stemming from ring closure around the thread (to generate the quasi[1]rotaxane **4**) and outside of the thread (to generate the non-interlocked conformer **4'**). Fortunately, separation of the two compounds using column chromatography was possible, and we could isolate the suspected quasi[1]rotaxane **4** in 16% yield over two steps (starting from free boronic acid **1** and thread **2**). The interlocked nature of **4** was clear already from its physical properties, as the compound was fully stable to chromatographic purification despite the hydrolytically sensitive boronic ester moiety.

^{1}H-NMR analysis showed full consumption of the external alkene protons r_{12}/r_{13} from **3** and the characteristic change in both shift and splitting pattern (m to t) of the internal alkene proton r_{11}, corresponding to the ring-closed metathesis product (Figure 1).

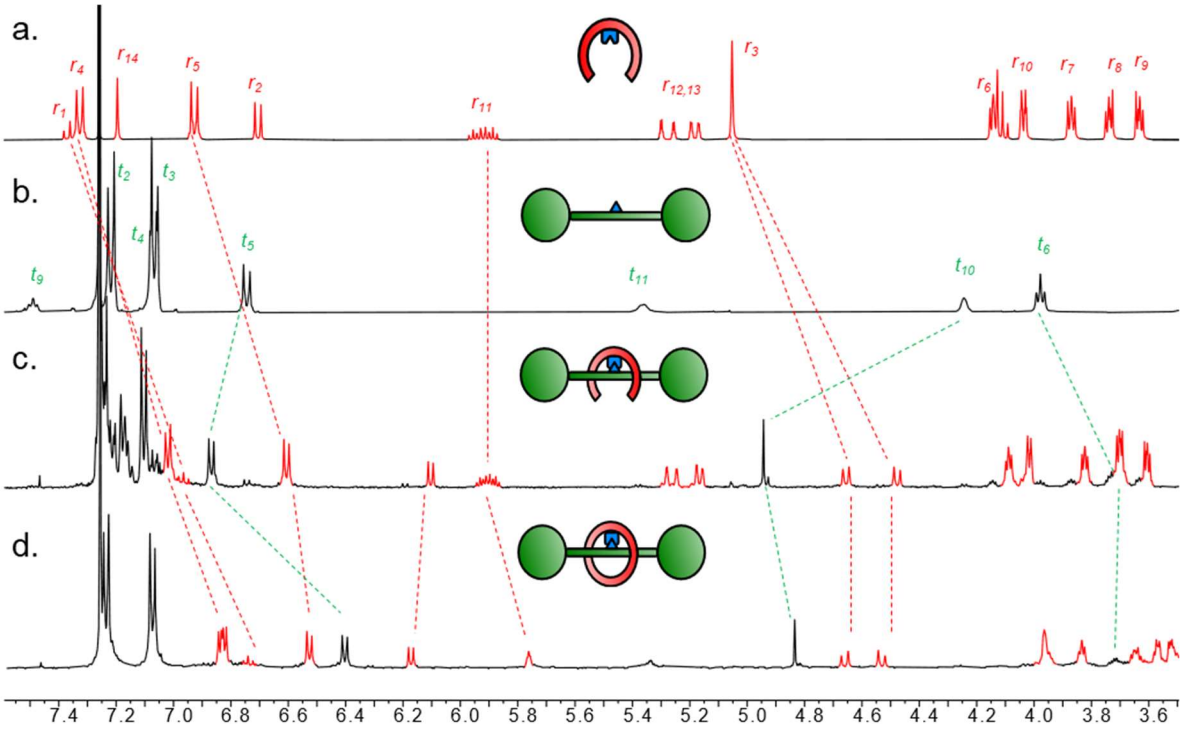

Figure 1. Partial ^{1}H-NMR spectra (500 MHz, $CDCl_3$, 298 K) of a) boronic acid pincer ligand **1**; b) tartrate-derived thread **2**; c) boronic ester condensation product **3** (89% conversion); d) quasi[1]rotaxane **4**.

Large upfield shifts for peaks corresponding to protons on the arms of the pincer receptor (r_3, r_4, r_5) as well as the thread (t_5, t_8) indicated the ring closing event produced a tight conformation with close association to the thread, in line with the expected quasi-interlocked conformation.

From this NMR analysis, we could now assign compound **4** as the minor product in the crude reaction mixture. A higher quantity of the suspected exo-macrocyclic conformer **4'** was, correspondingly, also observed. Attempts to isolate this molecule in pure form were fruitless, as **4'** hydrolyzed readily during chromatographic purification attempts or after being dissolved in wet organic solvents. Through rapid silica flash column chromatography we could isolate a mixture of **4'** together with the hydrolysis products, thread **2** and boronic-acid macrocycle **6** (Figure S5-S6).[26] Interestingly, macrocycle **6** could not be synthesized by direct RCM of ligand **1**, as this only produced degradation products. This methodology is the only method we have been able to find to obtain **6** as a reference compound.

In contrast to some previously used covalent templates[9], the boronic ester functionality is labile and requires only mild conditions to dissociate. Indeed, quasi[1]rotaxane **4** was found to slowly equilibrate to the free [2]rotaxane **5** when left in water-saturated $CDCl_3$ under ambient conditions. After several days, an equilibrium position of 70:30 between **5** and **4** was established (Figure 2). Considering the effective molarity between diol and boronic acid in **5**, the shift of the equilibrium position towards

hydrolysis product is somewhat unexpected and indicates that the boronic acid state is strongly favored over ester.

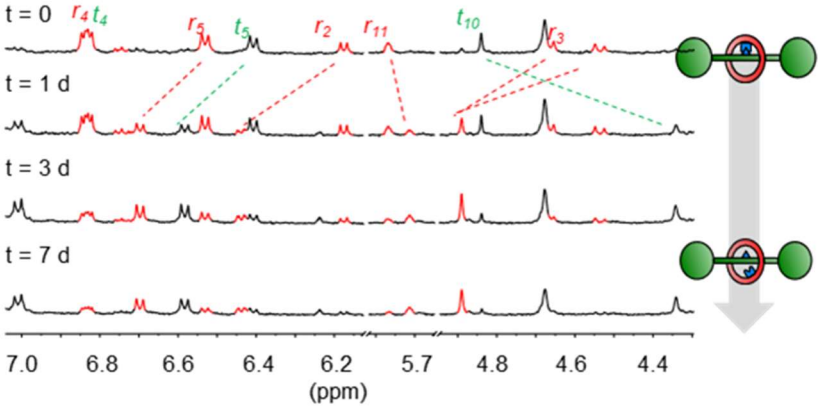

Figure 2. Partial ^{1}H-NMR spectra (500 MHz, $CDCl_3$, 298 K) showing gradual hydrolysis of **4** into [2]rotaxane **5**.

In contrast, the non-interlocked nature of **4'** was obvious from its chemical stability. Upon being left in wet $CDCl_3$ for 24 h, **4'** had dissociated to free **2** and macrocycle **6**, with >95% conversion to these products being observed after 48 h (Figure S5). By condensing the free thread **2** and macrocycle **6** under similar conditions to formation of the condensation complex **3**, we could also regenerate **4'** *in situ* (Figure S6).

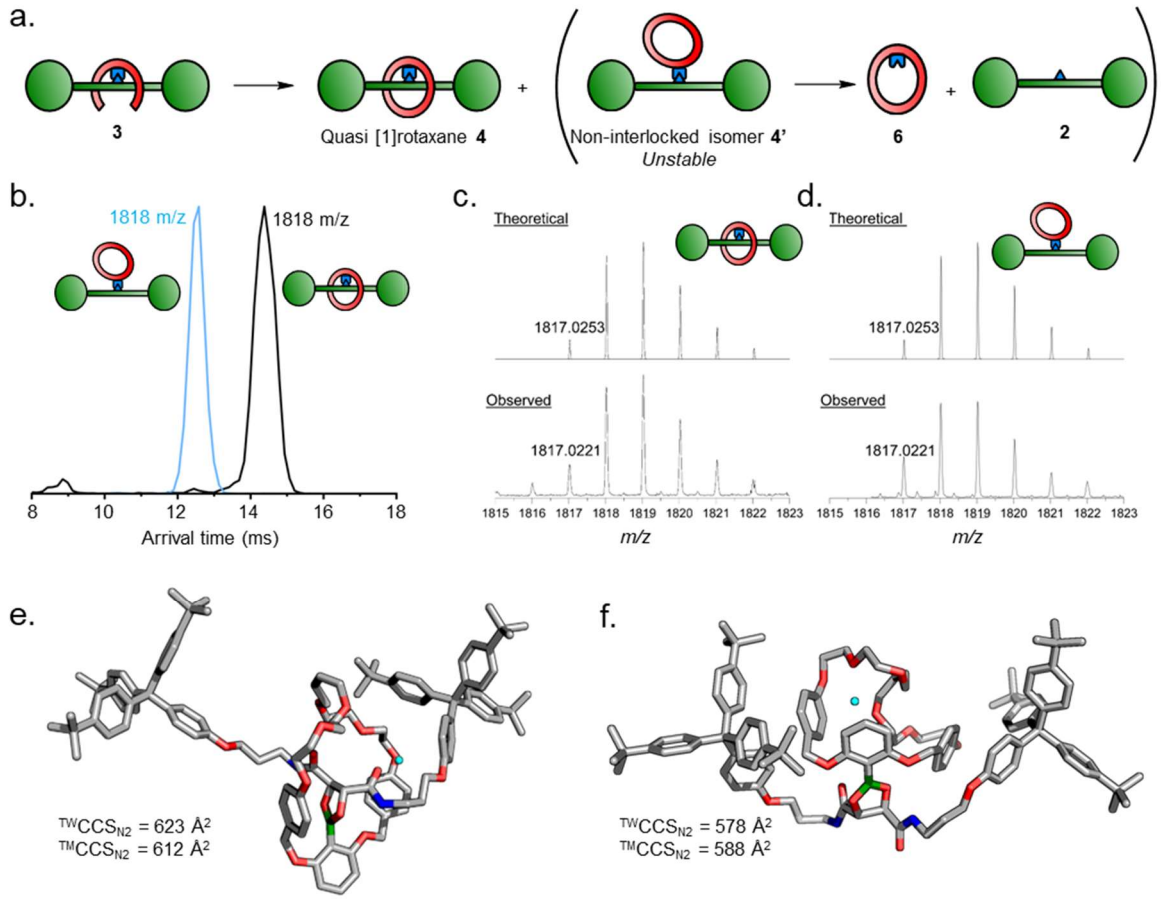

Figure 3. a) Scheme of ring-closing reaction to generate isomers **4** and **4'**, as well as the degradation of **4'** into macrocycle **6** and thread **2**. b) Overlapped TW-IMS measurements of **4** and **4'**. c) HRMS isotopic distribution for **4**. d) HRMS isotopic distribution for **4'**. e,f) HF-3c molecular models for e) [**4**•Na]$^+$ and f) [**4'**•Na]$^+$ used for calculation of theoretical collisional cross sections ($^{TM}CCS_{N2}$) and comparison with experimental collisional cross section values ($^{TW}CCS_{N2}$). Na^+ ion shown in cyan.

Isomers **4** and **4'** were also further analyzed via tandem mass spectrometry. The isolated samples were analyzed by traveling wave ion mobility mass spectrometry[27] (TW-IMS), which showed different arrival times for **4** (14.4 ms) and **4'** (12.5 ms) (Figure 3b, Table S2).[28] Experimental collision cross section ($^{TW}CCS_{N2}$) values, determined via a polyalanine calibrant (full detail in supporting information), were calculated to be 623 ± 3 and 578 ± 4 Å^2, for **4** and **4'**, respectively. Theoretical collisional cross section ($^{TM}CCS_{N2}$) of HF-3c optimised structures of **4** and **4'** (612 and 588 Å^2, respectively) were in good agreement with the experimental values (Figure 3e,f).[29]

We further used collision induced dissociation (CID) mass spectrometry experiments to investigate the nature of the linkage between the ring and thread components in the RCM products by following the fragmentation of the hydrolysis products (Figure S9-10). Starting from compound **4'**, hydrolysis was induced by dissolving the sample in 4:1 MeCN/H_2O mixture and incubating for 1 h before measuring. We detected the hydrolysis complex [**4'**•2H_2O] (or [**2•6**]) in the MS and subsequently isolated this peak for fragmentation. This complex between free ring **6** and thread **2** dissociated readily under CID conditions, with essentially full dissociation already at 20 V, indicating that this species is held together only through weaker interactions such as H-bonds rather than a mechanical bond. By incubating **4** under the same hydrolysis conditions, free [2]rotaxane **5** was then observed in the mass spectrometer (*m/z* 1854) and was selected for fragmentation via CID. Much higher collision voltages (>70 V) were required to induce fragmentation of **5** which interestingly dissociated via a double condensation to re-form the quasi[1]rotaxane **4**. Upon further increasing the collision voltage to 90 V, a second competing channel was also observed with dissociation of wheel and axle, likely by breaking one of the benzyl ether groups in the wheel. Even higher collision voltages were needed for fragmentation of **4** and **4'** where no specific thread/ring fragments were observed, as expected for entirely covalently linked molecules (Figure S11-S12). These measurements lend strong support to our interpretation that **5** is a mechanically interlocked molecule.

Quasi[1]rotaxane **4** is assembled through a boronic ester linkage. One advantage of boronic esters in organic chemistry is their versatility as synthetic handles. We hence tried exposing **4** to different derivatization conditions (Figure 4). As previously mentioned, free [2]rotaxane **5** is accessed through exposure to water-saturated $CDCl_3$ over extended time periods. Addition of strong acids (such as H_2SO_4 and HCl) mainly led to ring cleavage (likely via benzyl ether dissociation) and we could only observe small amounts if protodeboronylation rotaxane via ESI-HRMS (with only thread **2** isolable after workup). We then tried to oxidize the boronic ester with H_2O_2/NaOH to obtain a phenol, but this unexpectedly also led to cleavage of the macrocycle, liberating the free thread in 87% yield (Figure S7). Finally, we found that the phenol [2]rotaxane derivative could be accessed by omitting the base in the oxidation step. Dissolving compound **4** in a 1:1 THF/H_2O mixture with H_2O_2 for 1 h induced transformation to phenol rotaxane **7** in 67% isolated yield (Spectrum S41-S46, S9). This demonstrates we can selectively address the quasi[1]rotaxane scaffold in three different ways – macrocycle cleavage, thermodynamic ring-thread equilibration and derivatization of the macrocycle to obtain kinetically trapped [2]rotaxane **7**.

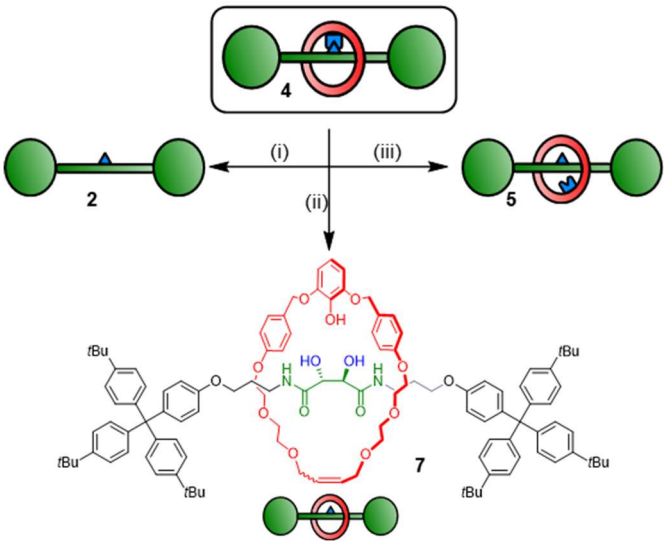

Figure 4. Derivatization of quasi[1]rotaxane **4**. Reagents and conditions: (i) H_2O_2, NaOH, THF/H_2O 1:1, RT, 1 h, 87%. (ii) H_2O_2, THF/H_2O 1:1, RT, 1 h, 67%. (iii) H_2O, $CDCl_3$, RT, 7 d (equilibrium yield 70%).

CONCLUSIONS

In summary, we have demonstrated that dynamic covalent bonds formed between boronic acids and vicinal diols can template rotaxane formation. The dynamic linkage brings the two components together in space, and by designing the boronic acid to be V-shaped we obtain preorganization for closure over the thread to obtain interlocked products. The isolated quasi[1]rotaxane is chemically stabilized from the mechanical bond, and could be derivatized in several ways through judicious choice of conditions. Though it is clear that the system can be optimized for both synthetic efficiency and compatibility with aqueous conditions, this nevertheless constitutes a proof-of-concept for the use of the biologically relevant vicinal diol motif as templates for mechanical bond formation. The use of dynamic covalent bonds for this purpose is critical, as bond cleavage in this system is facile and efficient, entirely circumventing the stabilizing "catenand effect" that has hindered template removal in previous examples of covalently templates MIMs.[9] Future boron pincers need to improve condensation conditions for formation of the initial assembly, the selectivity of the ring closure in favor of more interlocked product and increase the water stability of the system. Still, this work will be useful as a starting point for using natural biomolecules as threads for rotaxanes. This would mean the mechanical bond could be incorporated in biomolecules such as carbohydrates, RNA and polyhydroxylated natural products to modulate physical properties and give useful functions. While this study still requires compounds soluble in organic solvents, we believe this class of molecules could have future impact as building blocks for rotaxane biosensors and therapeutics.[2a]

ASSOCIATED CONTENT

Supporting Information. Experimental procedures, optimization data, NMR analysis and mass spectra (PDF). This material is available free of charge via the Internet.

AUTHOR INFORMATION

Corresponding Author

* Correspondence to: fresch@kth.se

Funding Sources

Swedish Research Council (2020-04225), Carl Tryggers Stiftelse (21:1584), Stiftelsen Olle Engkvist Byggmästare (215-0407), Magnus Bergvalls stiftelse, Wenner-Gren Stiftelserna (UPD2021-0106), and the H2020-MSCA-ITN project NOAH (765297).

Notes

The authors declare no competing financial interest.

ACKNOWLEDGMENT

FS gratefully acknowledges financial support from the Swedish Research Council (grant number 2020-04225), Carl Tryggers Stiftelse (21:1584), Stiftelsen Olle Engkvist Byggmästare (215-0407), Magnus Bergvalls stiftelse and the KTH Royal Institute of Technology. SD thanks Wenner-Gren Stiftelserna for an individual postdoctoral fellowship (UPD2021-0106). DLS thanks the European Union through the NOAH project (H2020-MSCA-ITN project Ref. 765297) and FU Berlin for funding. Support for measurements by the BioSupraMol core facility at FU Berlin is gratefully acknowledged.

ABBREVIATIONS

$^{TW}CCS_{N2}$, experimental collisional cross section; $^{TM}CCS_{N2}$, theoretical experimental collisional cross section calculated using the trajectory method; CID, collision induced dissociation; ESI-HRMS, electrospray ionization high resolution mass spectrometry; MIM, mechanically interlocked molecule; RCM, ring closing metathesis; RT, room temperature; TW-IMS, travelling wave ion mobility mass spectrometry.

REFERENCES

(1) (a) Bruns, C. J.; Stoddart, J. F. *The Nature of the Mechanical Bond: From Molecules to Machines*, Wiley-VCH, **2016**; b) van Dongen, S. F. M.; Cantekin, S.; Elemans, J. A. A. W.; Rowan, A. E.; Nolte, R. J. M. Functional interlocked systems. *Chem. Soc. Rev*, **2014**, *43*, 99–122; c) Erbas-Cakmak, S.; Leigh, D. A.; McTernan, C. T.; Nussbaumer, A. L. Artificial Molecular Machines. *Chem. Rev*. **2015**, *115*, 10081–10206; d) Ashbridge, Z.; Fielden, S. D. P.; Leigh, D. A.; Pirvu, L.; Schaufelberger, F.; Zhang, L. Knotting matters: orderly molecular entanglements. *Chem. Soc. Rev*. **2022**, *51*, 7779–7809; e) Heard, A.W.; Goldup, S.M. Simplicity in the design, operation, and applications of mechanically interlocked molecular machines. *ACS Cent. Sci*. **2020**, *6* 117–128.

(2) a) Beeren, S.; McTernan, C. T.; Schaufelberger, F. The Mechanical Bond in Biological Systems. *Chem*, **2023**, *9*, 1378–1412; b) Pairault, N.; Barat, R.; Tranoy-Opalinski, I.; Renoux, B.; Thomas, M.; Papot, S. Rotaxane-based architectures for biological applications. *C. R. Chimie,* **2016**, *19*, 103–112; c) Riebe, J.; Niemeyer, J. Mechanically Interlocked Molecules for Biomedical Applications. *Eur. J. Org. Chem*. **2021**, 5106–5116; d) Lim, N. C. H.; Jackson, S. E. Molecular knots in biology and chemistry. *J. Phys.: Condens. Matter*, **2015**, 27, 354101.

(3) a) Kench, T.; Summers, P. A.; Kuimova, M. K.; Lewis, J. E. M.; Vilar, R. Rotaxanes as Cages to Control DNA Binding, Cytotoxicity, and Cellular Uptake of a Small Molecule. *Angew. Chem. Int. Ed.* **2021**, 10928–10934; b) Barat, R.; Legigan, T.; Tranoy-Opalinski, I.; Renoux, B.; Péraudeau, E.; Clarhaut, J.; Poinot, P.; Fernandes, A. E.; Aucagne, V.; Leigh, D. A.; Papot, S. A mechanically interlocked molecular system programmed for the delivery of an anticancer drug. *Chem. Sci.* **2015**, 2608–2613.

(4) Baumes, J. M.; Gassensmith, J. J.; Giblin, J.; Lee, J.-J.; White, A. G.; Culligan, W. J.; Leevy, W. M.; Kuno, M.; Smith, B. D. Storable, thermally activated, near-infrared chemiluminescent dyes and dye-stained microparticles for optical imaging. *Nat. Chem.* **2010**, *2*, 1025–1030.

(5) Acevedo-Jake, A.; Ball, A. T.; Galli, M.; Kukwikila, M.; Denis, M.; Singleton, D. G.; Tavassoli, A.; Goldup, S. M. AT-CuAAC Synthesis of Mechanically Interlocked Oligonucleotides. *J. Am. Chem. Soc.* **2020**, 5985–5990.

(6) Bao, X.; Isaacsohn, I.; Drew, A. F.; Smithrud, D. B. Determining the Intracellular Transport Mechanism of a Cleft−[2]Rotaxane. *J. Am. Chem. Soc.* **2006**, *128*, 12229–12238.

(7) a) Slack, C. C.; Finbloom, J. A.; Jeong, K.; Bruns, C. J.; Wemmer, D. E.; Pines, A.; Francis, M. B. Rotaxane probes for protease detection by ^{129}Xe hyperCEST NMR. *Chem. Commun.* **2017**, *53*, 1076–1079; b) Klass, S. H.; Truxal, A. E.; Fiala, T. A.; Kelly, J.; Nguyen, D.; Finbloom, J. A.; Wemmer, D. E.; Pines, A.; Francis, M. B. Rotaxane Probes for the Detection of Hydrogen Peroxide by ^{129}Xe HyperCEST NMR Spectroscopy. *Angew. Chem. Int. Ed.* **2019**, *58*, 9948–9953.

(8) For examples of small-molecule MIMs with integrated biological functionalities, see a) Song, Y.; Schaufelberger, F.; Ashbridge, Z.; Pirvu, L.; Vitorica-Yrezabal, I. J.; Leigh, D. A. Effects of turn-structure on folding and entanglement in artificial molecular overhand knots. *Chem. Sci*. **2021**, *12*, 1826–1833; b) Schröder, H. V.; Zhang, Y.; Link, A. J. Dynamic covalent self-assembly of mechanically interlocked molecules solely made from peptides. *Nat. Chem.* **2021**, *13*, 850–857; c) Fernandes, A.; Viterisi, A.; Coutrot, F.; Potok, S.; Leigh, D. A.; Aucagne, V.; Papot, S. Rotaxane-Based Propeptides: Protection and Enzymatic Release of a Bioactive Pentapeptide. *Angew. Chem. Int. Ed.* **2009**, *48*, 6443–6447; d) Blankenship, J. W. Dawson, P. E. Threading a peptide through a peptide: protein loops, rotaxanes, and knots. *Protein Sci.* **2007**, *16*, 1249–1256; e) Yamamoto, M.; Takeuchi, M.; Shinkai, S. Oligosaccharide binding to a boronic-acid-appended phenanthroline·Cu(I) complex which creates superstructural helicates and catenates. *Tetrahedron*, **2002**, *58*, 7251–7258; f) Echavarren, J.; Gall, M. A. Y.; Haertsch, A.; Leigh, D. A.; Spence, J. T. J.; Tetlow, D. J.; Tian, C. Sequence-Selective Decapeptide Synthesis by the Parallel Operation of Two Artificial Molecular Machines. *J. Am. Chem. Soc.* **2021**, *143*, 5158–5165; g) Coutrot, F.; Busseron, E. A New Glycorotaxane Molecular Machine Based on an Anilinium and a Triazolium Station. *Chem. Eur. J*. **2008**, *14*, 4784–4787.

(9) Cornelissen, M. D.; Pilon, S.; van Maarseveen, J. H. Covalently Templated Syntheses of Mechanically Interlocked Molecules. *Synthesis,* **2021**, *53*, 4527–4548.

(10) For examples of covalently templated MIMs, see a) Steemers, L.; Wanner, M. J.; Lutz, M.; Hiemstra, H.; van Maarseveen, J. H. Synthesis of spiro quasi[1]catenanes and quasi[1]rotaxanes via a templated backfolding strategy. *Nat. Commun*. **2017**, *8*, 15392; b) Schweez, C.; Shushkov, P.; Grimme, S.; Höger, S. Synthesis and Dynamics of Nanosized Phenylene–Ethynylene–Butadiynylene Rotaxanes and the Role of Shape Persistence. *Angew. Chem. Int. Ed.* **2016**, *55*, 3328–3333; c) Pilon, S.; Ingemann Jørgensen, S.; van Maarseveen, J. H. Covalent [2]Catenane and [2]Rotaxane Synthesis via a δ-Amino Acid Template. *ACS Org. Inorg. Au,* **2021**, *1*, 37–42; d) Steemers, L.; Wanner, M. J.; van Leeuwen, B. R. C.; Hiemstra, H.; van Maarseveen, J. H. Attempted [2]Catenane Synthesis via a Quasi[1]catenane by a Templated Backfolding Strategy. *Eur. J. Org. Chem.* **2018**, 874–878; e) Pilon, S.; Jorgensen, S. I.; van Maarseveen, J. H. [2]Catenane Synthesis via Covalent Templating. *Chem. Eur. J.* **2021**, *27*, 2310–2314; f) Bu, A.; Zhao, Y.; Xiao, H.; Tung, C.-H.; Wu, L.-Z.; Cong, H. A Conjugated Covalent Template Strategy for All-Benzene Catenane Synthesis. *Angew. Chem. Int. Ed.* **2022**, *61*, e202209449; g) Segawa, Y.; Kuwayama, M.; Hijikata, Y.; Fushimi, M.; Nishihara, T.; Pirillo, J.; Shirasaki, J.; Kubota, N.; Itami, K. All-benzene catenane and trefoil knot. *Science*, **2019**, *365*, 272–276; h) Ünsal, Ö.; Godt, A. Synthesis of a [2]catenane with functionalities and 87-membered rings. *Chem. Eur. J.* **1999**, *5*, 1728–1733; i) Kameta, N.; Hiratani, K.; Nagawa, Y. A novel synthesis of chiral rotaxanes via covalent bond formation. *Chem. Commun*. **2004**, *4*, 466–467.

(11) Schill, G.; Lüttringhaus, A. The Preparation of Catena Compounds by Directed Synthesis. *Angew. Chem. Int. Ed. Engl*., **1964**, *3*, 546–547.

(12) a) Schaufelberger, F.; Timmer, B. J. J.; Ramström, O. *Principles of Dynamic Covalent Chemistry,* in *"Dynamic Covalent Chemistry: Principles, Reactions and Applications"* (eds. Zhang, W.; Jin, Y.), **2017**, Wiley-VCH; b) Jin, Y.; Yu, C.; Denman, R. J.; Zhang, W. Recent advances in dynamic covalent chemistry. *Chem. Soc. Rev.* **2013***, 42*, 6634–6654;

(13) For a recent review on the topic see a) Yu, J.; Gaedke, M.; Schaufelberger, F. Dynamic Covalent Chemistry for Synthesis and Co-conformational Control of Mechanically Interlocked Molecules. *Eur. J. Org. Chem*. **2023**, *26*, e202201130. For examples of dynamic covalent chemistry for MIM synthesis, see b) Kawai, H.; Umehara, T.; Fujiwara, K.; Tsuji, T.; Suzuki, T. Dynamic covalently bonded rotaxanes cross-linked by imine bonds between the

axle and ring: inverse temperature dependence of subunit mobility. *Angew. Chem. Int. Ed.* **2006**, *45*, 4281–4286; c) Hoshino, S.; Ono, K.; Kawai, H. Ring-Over-Ring Deslipping From Imine-Bridged Heterorotaxanes. *Front. Chem.* **2022**, *10*, 885939; d) Kandrnalova, M.; Kokan, Z.; Havel, V.; Nečas, M.; Šindelař, V. Hypervalent Iodine Based Reversible Covalent Bond in Rotaxane Synthesis. *Angew. Chem. Int. Ed.* **2019**, *58*, 18182–18185; e) Borodin, O.; Shchukin, Y.; Robertson, C. C.; Richter, S.; von Delius, M. Self-Assembly of Stimuli-Responsive [2]Rotaxanes by Amidinium Exchange. *J. Am. Chem. Soc.* **2021**, *143*, 16448–16457.

(14) a) Peters, J. A. Interactions between boric acid derivatives and saccharides in aqueous media: Structures and stabilities of resulting esters. *Coord. Chem. Rev*. **2014**, *268*, 1–22; b) Springsteen, G.; Wang, B. A detailed examination of boronic acid–diol complexation. *Tetrahedron*, **2002**, *58*, 5291–5300; c) Sun, X.; Chapin, B. M.; Metola, P.; Collins, B.; Wang, B.; James, T. D.; Anslyn, E. V. The mechanisms of boronate ester formation and fluorescent turn-on in ortho-aminomethylphenylboronic acids. *Nat. Chem.* **2019**, *11*, 768–778; d) Bull, S. D.; Davidson, M. G.; Van den Elsen, J. M. H.; Fossey, J. S.; Jenkins, A. T. A.; Jiang, Y.-B. Kubo, Y.; Marken, F.; Sakurai, K.; Zhao, J.; James, T. D. Exploiting the reversible covalent bonding of boronic acids: recognition, sensing, and assembly. *Acc. Chem. Res*. **2013**, *46*, 312–326.

(15) a) Davis, A. P. Biomimetic carbohydrate recognition. *Chem. Soc. Rev.* **2020**, *49*, 2531–2545; b) Williams, G. T.; Kedge, J. L.; Fossey, J. S. Molecular Boronic Acid-Based Saccharide Sensors. *ACS Sensors*, **2021**, *6*, 1508–1528.

(16) a) McClary, C. A.; Taylor, M. S. Applications of organoboron compounds in carbohydrate chemistry and glycobiology: analysis, separation, protection, and activation. *Carbohydr. Res.* **2013**, *381*, 112–122; b) Estrada, C. D.; Ting Ang, H.; Vetter, K.-M.; Ponich, A. A.; Hall, D. G. Enantioselective Desymmetrization of 2-Aryl-1,3-propanediols by Direct O-Alkylation with a Rationally Designed Chiral Hemiboronic Acid Catalyst That Mitigates Substrate Conformational Poisoning. *J. Am. Chem. Soc*. **2021**, *143*, 4162–4167.

(17) a) Röttger, M.; Domenech, T.; van der Weegen, R.; Breuillac, A.; Nicolaÿ, R.; Leibler, L. High-performance vitrimers from commodity thermoplastics through dioxaborolane metathesis. *Science*, **2017**, *356*, 62–65; b) Cromwell, O. R.; Chung, J.; Guan, Z. Malleable and Self-Healing Covalent Polymer Networks through Tunable Dynamic Boronic Ester Bonds. *J. Am. Chem. Soc*. **2015**, *137*, 6492–6495.

(18) Hong, S. H.; Shin, M.; Park, E.; Ryu, J. H.; Burdick, J. A.; Lee, H. Alginate-Boronic Acid: pH-Triggered Bioinspired Glue for Hydrogel Assembly. *Adv. Funct. Mater*. **2020**, *30*, 1908497.

(19) a) Stoltenberg, D., Lüthje, S., Winkelmann, O., Näther, C., Lüning, U. Tetraols as Templates for the Synthesis of Large endo-Functionalized Macrocycles. *Eur. J. Org. Chem.* **2011**, 5845–5859; b) Lüthje, S., Bornholdt, C., Lüning, U. Polyols as Templates for the Synthesis of Macrocycles from Boronic Acid Building Blocks. *Eur. J. Org. Chem*. **2006**, 909–915; c) Stoltenberg, D., Lüning, U. Macrocycle synthesis by trimerization of boronic acids around a hexaol template, and recognition of polyols by resulting macrocyclic oligoboronic acids. *Org. Biomol. Chem.* **2013**, *11*, 5109–5116; d) Ono, K.; Onodera, S.; Kawai, H. Boroxine template for macrocyclization and postfunctionalization. *Chem. Commun.* **2022**, *58*, 12544–12547; e) Içli, B.; Christinat, N.; Tönnemann, J.; Schüttler, C.; Scopelliti, R.; Severin, K. Synthesis of Molecular Nanostructures by Multicomponent Condensation Reactions in a Ball Mill *J. Am. Chem. Soc*. **2009**, *131*, 3154–3155.

(20) For examples were boron is directly used for assembly, see a) Hicguet, M.; Mongin, O.; Roisnel, T.; Berrée, F.; Trolez, Y. Threading a linear molecule through a macrocycle thanks to boron. *ChemRxiv*, **2023**, 10.26434/chemrxiv-2023-707rs-v2; b) Zhang, G.; Presly, O.; White, F.; Oppel, I. M.; Mastalerz, M. A Shape-Persistent Quadruply Interlocked Giant Cage Catenane with Two Distinct Pores in the Solid State. *Angew. Chem. Int. Ed.* 2014, *53*, 5126–5130. For other examples of boron-containing MIMs, see: c) Christinat, N.; Scopelliti, R.; Severin, K. Boron-based rotaxanes by multicomponent self-assembly. *Chem. Commun*. **2008**, 3660–3662; d) Koyama, Y.; Matsumura, T.; Yui, T.; Ishitani, O.; Takata, T. Fluorescence Control of Boron Enaminoketonate Using a Rotaxane Shuttle. *Org. Lett.* **2013**, *15*, 4686–4689; e) Rémy, M.; Nierengarten, I.; Park, B.; Holler, M.; Hahn, U.; Nierengarten, J.-F. Pentafluorophenyl Esters as Exchangeable Stoppers for the Construction of Photoactive [2]Rotaxanes. *Chem. Eur. J.* **2021**, *27*, 8492–8499; f) Kage, Y.; Shimizu, S.; Kociok-Kohn, G.; Furuta, H.; Pantoş, G. D. Subphthalocyanine-Stoppered [2]Rotaxanes. *Org. Lett.* **2020**, *22*, 1096–1101, g) Nisanci, B.; Sahinoglu, S.; Tuner, E.; Arik, M.; Kani, I.; Dastana, A.; Bozdemir, Ö. A. Synthesis of an F-BODIPY [2]catenane using the chemistry of bis(dipyrrinato)metal complexes. *Chem. Commun*. **2017**, *53*, 12418–12421; h) Nakamura, T.; Yamaguchi, G.; Nabeshima, T. Unidirectional Threading into a Bowl-Shaped Macrocyclic Trimer of Boron-Dipyrrin Complexes through Multipoint Recognition. *Angew. Chem. Int. Ed*. **2016**, *55*, 9606–9609.

(21) Smith and co-workers have designed a range of fluorescent dyes with protective “arms” that resemble our condensation product, see: a) Li, D.-H.; Gamage, R. S.; Oliver, A. G.; Patel, N. L.; Usama, S. M.; Kalen, J. D.; Schnermann, M. J.; Smith, B. D. Doubly Strapped Zwitterionic NIR-I and NIR-II Heptamethine Cyanine Dyes for Bioconjugation and Fluorescence Imaging. *Angew. Chem. Int. Ed.* **2023**, *62*, e202305062; b) Li, D.-H.; Schreiber, C. L.; Smith, B. D. Sterically Shielded Heptamethine Cyanine Dyes for Bioconjugation and High Performance Near-Infrared Fluorescence Imaging. *Angew. Chem. Int. Ed*. **2020**, *59*, 12154–12161; c) Schreiber, C. L.; Li, D.-H.; Smith, B. D. High-Performance Near-Infrared Fluorescent Secondary Antibodies for Immunofluorescence. *Anal. Chem.* **2021**, *93*, 3643–3651; d) Li, D.-H.; Gamage, R. S.; Smith, B. D. Sterically Shielded Hydrophilic Analogs of Indocyanine Green. *J. Org. Chem.* **2022**, *87*, 11593–11601.

(22) Condensation yield had a large variability under repeat conditions or even in glovebox settings. Attempts to increase condensation yield by switching solvents and concentrations failed, as did addition of a range of drying agents and use of a Dean-Stark apparatus. Instead of increased conversion to boronic ester, we observed boroxazine trimerization of the ligand under such conditions, indicating that the desired cleft-receptor **3** is likely a metastable reaction product.

(23) Valenzuela, S. A.; Howard, J. R.; Park, H. M.; Darbha, S.; Anslyn, E. V. ^{11}B NMR Spectroscopy: Structural Analysis of the Acidity and Reactivity of Phenyl Boronic Acid–Diol Condensations. *J. Org. Chem*. **2022**, *87*, 15071–15076.

(24) Guidry, E.N.; Cantrill, S.J.; Stoddart, J. F.; Grubbs, R. H. Magic ring catenation by olefin metathesis. *Org. Lett.* **2005**, *7*, 2129–2132.

(25) Li, A.; Tan, Z.; Hu, Y.; Lu, Z.; Yuan, J.; Li, X.; Xie, J.; Zhang, J.; Zhu, K. Precise Control of Radial Catenane Synthesis via Clipping and Pumping, *J. Am. Chem. Soc.* **2022**, *144*, 2085–2089.

(26) Taladhar, S. M.; D'Silva, C. The synthesis of 2-borono-1,3-xylyl crown ethers. *Tetrahedron Lett.* **1992**, *33*, 265–268.
(27) a) Kalenius, E.; Groessl, M.; Rissanen, K. Ion mobility–mass spectrometry of supramolecular complexes and assemblies. *Nat. Rev. Chem*. **2019**, *3*, 4–14; b) Kruve, A.; Caprice, K.; Lavendomme, R.; Wollschläger, J. M.; Schoder, S.; Schröder, H. V.; Nitschke, J. R.; Cougnon, F. B. L.; Schalley, C. A. Ion Mobility Mass Spectrometry for the Rapid Determination of the Topology of Interlocked and Knotted Molecules. *Angew. Chem. Int. Ed*. **2019**, *58*, 11324–11328; c) Zimnicka M. M. Structural studies of supramolecular complexes and assemblies by ion mobility mass spectrometry. *Mass Spectrom. Rev*. **2023**, doi.org/10.1002/mas.21851.
(28) Analysis of the crude reaction mixture also yielded a mixture of species with both arrival times, in line with expectations.
(29) Sure, R.; Grimme, S. Corrected small basis set Hartree-Fock method for large systems. *J. Comput. Chem*. **2013**, 34, 1672–1685.